Inverse relationship between fractionated electrograms and atrial fibrosis in persistent atrial fibrillation: combined magnetic resonance imaging and high-density mapping

Amir S. Jadidi, Hubert Cochet, Ashok J. Shah, Steven J. Kim, Edward Duncan, Shinsuke Miyazaki, Maxime Sermesant, Heiko Lehrmann, Matthieu Lederlin, Nick Linton, et al.

Inverse Relationship between Fractionated Electrograms and Atrial Fibrosis in Persistent Atrial Fibrillation - A combined MRI and High Density Mapping

Amir S. Jadidi MD; Hubert Cochet MD; Ashok J Shah MD; Steven J. Kim MEEng; Edward Duncan MD; Shinsuke Miyazaki MD; Maxime Sermesant PhD; Heiko Lehrmann MD; Matthieu Lederlin MD; Nick Linton MEng MRCP; Andrei Forclaz MD; Isabelle Nault MD FRCPC; Lena Rivard MD; Matthew Wright MBBS, Ph.D; Xingpeng Liu MD; Daniel Scherr, MD; Stephen B. Wilton, MD; Laurent Roten, MD; Patrizio Pascale, MD; Nicolas Derval MD; Frédéric Sacher MD; Sebastien Knecht MD; Cornelius Keyl MD; Mélèze Hocini MD, Michel Montaudon MD; Francois Laurent MD; Michel Haïssaguerre MD, and Pierre Jais

Short Title: Impact of fibrosis on electrograms in Atrial Fibrillation

Word count: 5058

Corresponding Author:

Amir S. Jadidi

Hôpital Cardiologique du Haut-Lévêque

33604 Bordeaux-Pessac, France

Tel : + 33 668 19 91 43, Fax: + 33 5 57 65 68 96

Email: amir.s.jadidi@gmail.com

Introduction: Atrial fractionated electrograms (CFAE) are strongly related to slow anisotropic conduction. We evaluated the relationship between fibrosis imaged by delayed enhancement (DE) MRI and atrial electrograms in persistent atrial fibrillation.

Methods: Atrial high resolution MRI of 18 patients with persistent AF (11 long-persistent) was registered with the mapping geometry (NavX). DE areas were categorized as dense or patchy, depending on their DE content. Left atrial electrograms (Egm) during AF were acquired using a high-density 20-pole catheter (514+/-77 sites/map). Fractionation, organisation/regularity, local mean cycle length, and voltage were analysed with reference to DE.

Results: Patients with long-persistent vs persistent AF had larger LA surface area (134+/-38cm2 vs 98+/-9cm2, p=0.02), higher amount of atrial DE (70+/-16cm2 vs 49+/-10cm2, p=0.01), more CFAE extent (54+/-16cm2 vs 28+/-15cm2, p=0.02) and a shorter baseline AF cycle length (147+/-10ms vs 182+/-14ms, p=0.01). Continuous CFAE (CFEmean<80ms) occupied 38+/-19% of total LA surface area. Dense DE was detected at the left posterior LA. In contrast, the right posterior LA contained predominantly patchy DE. Most CFAE (48+/-14%) occurred at non-DE LA sites, followed by 41+/-12% CFAE at patchy DE and 11+/-6% at dense DE regions (p=0.005 and p=0.008 respectively). 19+/-6% CFAE sites occurred at border zones of dense DE.

Egms were less fractionated, with longer cycle length and lower voltage at dense DE vs non-DE regions: CFEmean: 97ms vs 76ms, p<0.0001; local cycle length: 153ms vs 143ms, p<0.0001; mean voltage: 0.63mV vs 0.86mV, p<0.0001.

Conclusions: Atrial fibrosis as defined by DE MRI is associated with slower and more organized electrical activity but with lower voltage than healthy atrial areas. Ninety percent of continuous CFAE sites occur at non-DE and patchy DE left atrial sites. These findings are of importance for the choice of ablation strategy in persistent AF.

Keywords: Atrial Fibrillation; Atrial delayed Enhancement, MRI, Atrial Fibrosis, Ablation, Complex Fractionated Atrial Electrogram (CFAE), Cycle length, Pulmonary vein isolation.

ABBREVIATIONS

aDE	Atrial DE
AF	Atrial Fibrillation
CFAE	Complex fractionated atrial electrogram

CFEmean	NavX algorithm that quantifies Egm fractionation
DE	Delayed enhancement
Egm	Electrogram
LA	Left Atrium
LAA	Left atrial appendage
RAA	Right atrial appendage
MRI	Magnetic Resonance Imaging
PVI	Pulmonary Vein Isolation
PAF	Persistent AF

Introduction:

Atrial fibrillation (AF) is the most common arrhythmia associated with substantial morbi-mortality in humans. The pulmonary veins (PV) are the main drivers of paroxysmal AF and their isolation by ablation is associated with restoration of sinus rhythm [1]. In (long-)persistent AF, PVs play a less prominent role than widespread structural and functional alterations in the atrial substrate, which lower the success rate of PVI alone. Therefore, ablation strategies targeting CFAE sites in addition to PVI have been shown to improve maintenance of sinus rhythm [2,3]. CFAE are associated with slow anisotropic conduction in experimental conditions [15,16,20]. They may also result from farfield signals arising from adjacent myocardium (double

counting), or from wave collision during AF [5,6], or rapid focal or re-entrant activity [17], preferentially at ganglionated plexus sites [18].

Histopathological studies in humans and canine models of persistent AF have reported extracellular matrix remodelling with fibrotic infiltration causing atrial dilatation [7,8]. Studies using gadolinium-enhanced MRI have described areas of DE in the atrial wall of patients with AF due to the presence of fibrosis. Recent clinical studies suggest that a high burden of atrial DE prior to ablation might be associated with poor post-ablation outcome [9]. This may be related to the impact of fibrosis on wave propagation during AF [8]. We assessed the role of atrial fibrosis on the characteristics of atrial electrograms during AF.

Methods

Patients

We prospectively enrolled 18 consecutive patients referred to our centre between June and September 2010 for persistent AF ablation. Our institutional review board approved the study, and each of the patients provided a written informed consent. Inclusion criteria were the presence of persistent (lasting > 7 days) or long-persistent (lasting >12 months) AF without history of previous ablation. Exclusion criteria were contraindications to MRI (metallic implants, claustrophobia, etc.) and the presence of atrial thrombi on pre-procedural trans-oesophageal echocardiography. Among 18 patients (mean age 63+/-7yrs, range 47-70 yrs, 2 females), 11 had long-lasting persistent AF. Anti-arrhythmic medications were discontinued for 5 half-lives before the ablation procedure. All patients underwent cardiac MRI 1-2 days prior to the procedure. High density left atrial mapping was performed during AF, prior to ablation.

MRI

Image Acquisition

MRI studies were conducted on a 1.5 T clinical scanner (Avanto, Siemens Medical Solutions, Erlangen, Germany) equipped with a 32-channel cardiac coil. DE MRI was performed 15 minutes after the administration of 0.2 mmol/kg gadoterate dimeglumine (Dotarem, Guerbet, France). Imaging was acquired with the use of a 3-dimensional, inversion-recovery-prepared, respiration-navigated, ECG-gated, gradient-echo pulse sequence with fat-saturation. ECG gating was set to 50% of the mean RR interval in order to acquire signal in mid-diastole. Acquisition parameters were: voxel size 1.25x1.25x2.5mm (reconstructed to

0.625x0.625x2.5mm with in-plane interpolation), flip angle 22°, repetition time/echo time 5.4/2.3 ms, inversion time 260 to 320 ms (depending on the results of a previously acquired TI scouting sequence), parallel imaging with GRAPPA technique *R*=2, number of reference lines 44. Scan time ranged 5 to 10 minutes depending on patient's heart and respiratory rates.

Image Post-processing

Image post-processing was performed by 2 observers (HC, SK). Image processing was performed before the EP procedure and the observer was blinded to all EP data. Segmentation was performed with OsiriX 3.6.1 (Geneva, Switzerland). For modelling we used CardioViz3D (INRIA, Sophia Antipolis, France). LA wall was segmented manually by contouring the endocardial and epicardial borders of the atrium, including the pulmonary vein ostia and the first 2 cm of each PV. Areas of aDE were detected and segmented by performing a slice by slice histogram analysis with a semi-automatic signal threshold as described previously [9] (for details see Figure1). From the segmented images, the LA blood pool volume was quantified (corresponding to LA endocardial volume). Two series of binary images were produced for modelling purposes: the first one corresponding to the areas of atrial DE, and the second one corresponding to the blood pool volume, including pulmonary veins and coronary sinus to provide landmarks for subsequent registration with the NavX LA geometry. 3D meshes of LA blood pool volume and atrial DE volumes were computed using CardioViz3D and exported as XML into the NavX system (SJM, US). Delayed enhanced LA sites were differentiated in to (1) dense/continuous DE regions and (2) patchy/intermittent DE regions, if the DE was non-continuous and non-enhanced tissue was found in between the lately enhanced sites. We considered atrial tissue as dense/continuously enhanced if >90% of that regional atrial surface area contained DE. Patchy/intermittent DE was defined as inhomogeneous infiltration of atrial tissue by DE (DE content 20% to 70% of regional surface

area). If the atrial tissue did not contain any DE at MRI, it was qualified as non-DE area (see figures 1 and 4).

Atrial Fibrillation cycle length at baseline

In each patient, the baseline AF cycle length was measured in the LAA over 20 AF cycles during CFAE-mapping.

Electrophysiological Mapping

Co-registration of MRI and Electrophysiological data

After establishing a trans-septal access to LA, 50 IU/kg Heparin was given IV. LA geometry was acquired using a double-loop 20-pole catheter AFocus II HD (SJM, US). The LA geometry was carefully registered with the LA blood pool volume derived from MRI. This process was achieved by performing a point-by-point registration of 40-50 anatomical landmarks (PVs, LAA and CS; Figure 4). A decapolar catheter (Xtreme, ELA, France) was used as spatial reference.

Mapping of CFAE, analysis of surface areas with continuous CFAE vis-a-vis DE

CFAE maps were acquired using a 20-pole catheter (AFocus II HD) and the NavX (V8.0) system. Bipolar electrograms were filtered at 30 to 300 Hz and analysed to compute mean fractionation ("CFEmean" map) and bipolar voltage during an 8 second recording period at each site. For optimal detection of continuous CFAE using NavX CFEmean algorithm: minimum peak-to-peak electrogram voltage for detection was set at 0.08mV with a refractory

period setting of interval detection at 40 ms. [6,11] Continuous CFAE sites were defined as sites with CFEmean interval < 80ms [6], which, in our experience, corresponds to the continuous CFAE sites that are targeted for ablation [4]. Spatial relationship between continuous CFAE and the regions of atrial DE were quantified by manually contouring both areas, as well as the region of overlap (between continuous CFAE & dense DE and continuous CFAE & patchy DE), on the registered volume. Each of these surface areas were measured separately and expressed as a percentage of total LA area, total CFAE area, total dense DE area and total patchy DE area.

Analysis of Electrograms from dense DE, patchy DE and non-DE regions:

For the analysis of electrogram (Egm) characteristics at dense DE vs. patchy DE vs. non-DE, we exported Egms from each of these regions from the CFAE maps. The exported Egms were analysed according to their CFEmean value (8-second recording period), cycle length (1-second recording period) and mean voltage in AF (8-second recording period). For cycle length measurement, we analysed the subset of organised Egms, where the local cycle length could be clearly identified (green electrograms in figures 4B&D).

Quantification of Organized Electrograms at dense DE vs. patchy DE vs. non-DE

Bipolar Egms were scrutinized and categorized into organized or non-organized activity. Egms were considered non-organized, if fractionation led to the absence of isoelectric baseline, making local cycle length measurement impossible at that site (red electrograms in figure 4B&D). These non-organized Egms were then temporarily removed from the map. The remaining organized Egms where the measurement of AF cycle length was feasible were compared to the total number of mapped Egms in that region.

Percentage of organized Egms per region = number of organized Egms / (number of organized Egms + number of non-organized Egms) * 100. We calculated the "percentage of Egms with organized activity" at LA sites with DE vs. patchy DE vs. non-DE.

Atrial Fibrillation Ablation

Irrigated RF ablation (Thermocool, BW, CA) applied 25W on the posterior LA, 28W on the LA roof and anterior PV antrum. Patients with persistent AF (>7 days) underwent proximal PVI followed by electrical cardioversion, if AF persisted and linear lesions if atrial flutter was obtained.

Patients with long-persistent AF underwent stepwise ablation. PVI was followed by ablation of continuous CFAE (CFEmean <80ms) in the following order: LA roof, septum, inferior LA (facing the CS), lateral LA wall (at mitral isthmus region) and base of the LAA. CFAE at anterior LA were targeted prior to CFAE within the CS and at the posterior LA. The cycle lengths within the left and right atrial appendages were measured after each ablation step. If RAA-CL was shorter by >10ms than LAA-CL, further CFAE ablation was performed at rapid fractionated sites within the right atrium. If AF did not terminate during CFAE ablation, linear ablation at LA roof, lateral mitral isthmus including epicardial ablation within coronary sinus (at ≤25W) and cavotricuspid isthmus was performed. In case of AF persisting, patients were cardioverted electrically and PVI and bidirectional linear blocks were ascertained.

Statistical Analysis

Statistical analysis was performed using SPSS for Windows 16.0 (SPSS, Chicago, US). Continuous data are presented as mean ± standard deviation. In the absence of normal distribution, the non-parametric Mann-Whitney U Test was used for comparing the groups. As Egm characteristics (fractionation (CFEmean), cycle length and voltage) showed a positively skewed distribution, data were analysed using nonparametric tests. The Kruskal-Wallis one-way analysis of variance of ranks was performed to compare data of the three groups. Post hoc analyses were carried out using the two-sided Mann-Whitney test. Categorical data were compared between different groups using the Chi-square test. Pearson correlation coefficient was used to calculate correlation between the extent of delayed enhancement and AF cycle length. Exponential line fitting was chosen based on the equation: $y = ax^{b}$. The median with the first and third quartiles (Q1, Q3) is reported for skewed data with asymmetric distribution (figure 5A, 6A and C).

A P-value <0.05 was considered statistically significant. The alpha error level was corrected to 0.016 for triplicate performance of the Mann-Whitney test.

Results:

Among 18 persistent AF patients, there were 11 with long-persistent AF.

High density Mapping of CFAE

The CFAE-map density was 514+/-77 sites/patient (range 380-676; 2,93+/-0,79points/cm2), amounting to 9252 sites (electrograms) recorded in 18 patients, totally.

Left atrial size, extent of atrial DE and CFAE sites

A) Study population

Tables1&2 show the patient characteristics. The mean left atrial volume was 130+/-31ml, left atrial surface area was 119+/-39cm2 and the AF cycle length within the LAA was 153+/-15ms. We considered atrial tissue as dense/continuously enhanced if >90% of the regional surface area showed DE at MRI. Patchy/intermittent DE was defined as inhomogeneous enhancedment on MRI. The percentage of DE within the dense DE vs patchy DE areas was 96+/-4% vs. 37+/-12%, respectively ($p<0.0001$). Atrial regions without DE, were qualified as non-DE areas (figure 1&4).

In total, DE occupied 65+/-13cm2 (57+/-15%) and non-DE regions occupied 54+/-33cm2 (42+/-15%) of the LA area. The area of dense DE was smaller than that of the patchy DE: 16+/-4cm2 (14+/-5% of total LA surface) and 49+/-13cm2 (43+/-12% of total LA surface), $p<0.001$, respectively (figures 3A&C and 4A&C).

The total surface area of continuous CFAE was 42+/-18cm2 (38+/-19% of LA surface, figure 3A).

B) DE surface areas and electrical parameters in Long-persistent vs. persistent AF

Patients with long-persistent AF had larger LA surface area (134+/-38cm2 vs 98+/-9cm2, p=0.02), with greater amount of total atrial DE (70+/-16cm2 vs 49+/-10cm2, p=0.01) and more continuous CFAE surface area (54+/-16cm2 vs 28+/-15cm2, p=0.02, Figure2A), than persistent AF.

While the extent of dense DE was similar in patients with long-persistent and persistent AF (16,9+/-4cm2 vs 16.6+/-4.4cm2, p=0.88), the extent of patchy DE was higher in patients with long-persistent AF (53+/-14cm2 vs 34+/-9cm2, p=0.01).

Dense DE was consistently encountered in all patients on the left side of the posterior LA adjacent to the left PV ostia and within the track/path of the descending aorta (figure1C). The distribution of patchy DE was variable, although the right side of the posterior LA (towards the right PV ostia) showed patchy DE in all patients with long-persisting AF.

Baseline LAA AF cycle length was shorter in patients with long-persistent than persistent AF (147+/-10ms vs 182+/-14ms, p=0.01, figure 2A). The patients with a very short AF cycle length (<145ms) had a higher extent of total DE (71+/-7cm2), than the patients with cycle length >175ms (42+/-5cm2, p=0.01; figure 2B). In general, AF cycle length and the extent of atrial DE were inversely correlated (r= -0.74; figure 2C).

Analysis of the distribution of continuous CFAE vis-a-vis DE

Figure 3A illustrates the absolute surface areas of the LA, dense DE, patchy DE, non-DE and continuous CFAE sites. Figures 3B-E illustrates the relative extent of CFAE and DE:

Continuous CFAE sites occupied 38+/-19% of the LA area (3A,B). Dense and patchy DE occupied 14+/-5% and 43+/-12% of total LA surface, respectively. 42+/-15% of LA surface did not show any DE (non-DE area; 3C).

A minority of continuous CFAE sites occurred at dense DE regions (11+/-6% of CFAE sites), whereas most of it (48+/-14%) occurred at non-DE sites (p=0.005), followed by 41+/-12% at patchy DE regions (p=0.008, 3D, 4A-D). Notably, 19+/-6% of CFAE sites occurred at border zones of dense DE or within dense DE regions.

A minority (23+/-13%), of dense DE regions (4+/-5% of the LA surface) displayed continuous CFAE; figures 3E, 4 and 5B. The majority of dense DE regions showed organized electrical activity. On the other hand, 35+/-18% of patchy DE regions (15+/-12% of LA surface) (figure 3E) and notably, 46+/-27% of non-DE regions displayed continuous CFAE (19+/-8% of the LA surface); figure 3E.

Electrogram fractionation (CFAE) at LA sites with dense DE vs. patchy vs. non-DE sites

A lower degree of electrogram fractionation (with higher CFEmean values) was found at sites with dense DE (108+/-44ms) vs. patchy DE (87+/-34ms, p<0.0001) vs. non-DE regions (85.7+/-32ms, p<0.0001; figure 5A). Notably, 57% and 56% of Egms within patchy DE (figure 5B, green curve) and non-DE regions (pink curve) displayed continuous CFAE (CFEmean <80ms). In contrast, 33% of Egms within dense DE region showed continuous CFAE (Figure 5B, blue curve, p=0.009).

Electrogram Cycle length at LA sites with dense DE vs patchy DE vs non-DE

Dense DE areas showed slower and more organized electrical activity during AF than the other sites. The mean cycle length (CL) at sites with dense DE was 155+/-28ms vs. 148.6+/-28ms at patchy DE ($p<0.0001$) and 148.2+/-29.3ms at non-DE areas, ($p<0.0001$, figure 6A). There was no difference in AF cycle length at patchy DE vs. non-DE areas ($p=0.92$).

Distribution of organized electrical activity at dense DE vs. patchy DE vs. non-DE regions

A total of 9252 Egms were recorded among 18 patients included in the study (514+/-77 per patient). After qualitative analysis by visual inspection of 1-second recording period at each mapped site, 53.6% of all Egms were characterized as organized and 46.4% as non-organized. Organized Egms were more frequently observed at dense DE regions than other sites: 68% of recorded Egms at dense DE sites showed organized activity vs. 54% of Egms at patchy DE ($p<0.0001$) and 47% of Egms at non-DE sites ($p<0.0001$, figure 6B).

D) Mean electrogram voltage during AF at dense DE vs. patchy DE vs. non-DE sites

The global mean bipolar electrogram voltage during AF (8-second recording period) was 0.78+/-0.89mV. Electrograms at dense DE areas had significantly lower mean bipolar voltage (0.63+/-0.8mV) than those at patchy DE areas (0.86+/-1.09mV, $p<0.0001$) and non-DE regions (0.86+/-0.89mV, $p<0.0001$, figure 6C). There was no significant difference in bipolar Egm voltage at patchy DE vs. non-DE regions ($p=0.94$).

Atrial Fibrillation Ablation Results:

Continuous CFAE ablation (at CFEmean<80msec) prolonged AF cycle length within the LAA in 7/11 (64%) patients with long-persistent AF from mean 135ms to 190ms, $p<0.05$).

AF terminated into atrial tachycardia during CFAE ablation in 2/11 patients. Atrial tachycardias (1 roof dependent and 1 perimitral flutter) converted to sinus rhythm during linear ablation. CFAE ablation within the right atrium was necessary in 2 patients and resulted in prolongation of AF cycle length from mean 160ms to 210ms ($p<0.05$). All long-persistent AF patients had linear ablations at roof, mitral isthmus and cavo-tricuspid isthmus. AF freedom was achieved in 64% (7/11) patients with long persistent AF, after a mean FU period of 18+/-6 months and 1,7 procedures (range: 1-3).

AF freedom was achieved in 86% (6/7) patients with persistent AF after a mean FU period of 18+/-6 months and 1,1 procedures (range: 1-2).

Discussion:

This study analyzes the relationship between atrial fibrosis and electrogram characteristics (fractionation, cycle length, organisation and voltage) during human persistent atrial fibrillation. We provide correlation between the changing electrogram characteristics during atrial fibrillation and the varying extent of atrial fibrosis. Our initial hypothesis was that DE areas (atrial fibrosis) would be associated with more chaotic and fractionated electrical activity. This study demonstrates the opposite. We found 2 different types of fibrosis pattern in the atrial wall, as depicted at high-resolution cardiac delayed enhancement (DE) MRI: Fibrosis in patients with persistent AF may be homogeneous/dense or patchy, i.e. non-confluent (figure 1&4). These aspects are associated with distinct electrical characteristics.

Validation of scar imaging by MR

We used delayed Gadolinium enhancement at high resolution ECG- and respiration-gated cardiac MRI with a reconstructed voxel size of 0.625x0.625x2.5mm. As previously shown by

Oakes and collaborators using the same MRI sequence, regions of atrial DE correlated with regions of low voltage during sinus rhythm [9]. The correlation between DE and fibrosis has been shown for ventricular scar [13] by histo-pathological studies and in very recent reports also for atrial tissue. We used the same slice-based voxel intensity analysis that has been described by Oakes & Marrouche et al. for atrial DE detection and segmentation [9, 10] (figure 1). In order to get even higher specificity for atrial fibrosis and reduce noise detection, we considered voxel intensities equal or more than 4 standard deviations (SD) of the mean in-plane voxel internsity - instead of 2 or 3 in the studies of Oakes & Marrouche et al. - to qualify for pathological DE (figure 1). There have been controversies on the ability of DE MRI to image scar in the thin walled atrium. However, we do believe that the inverse correlation reported in our study between DE and CFAE validates scar imaging. If the segmentation of atrial DE areas was incorrect, no correlation with electrical activity would have been observed.

As expected, this study demonstrates that the patients with long-persistent AF have larger LA size with higher extent of atrial DE, larger continuous CFAE area and shorter AF cycle length than those with persistent AF (figure 2A). Patients with very short LAA-CL (<145ms) were found to have higher extent of total aDE (35-40% of LA surface) than patients with longer baseline AFCL (>170ms; 2B). Moreover, a negative correlation between the extent of aDE and baseline AFCL (r=-0.74; p=0.001; 2C) was found. These results demonstrate that the higher complexity of the fibrillating mechanisms/AF drivers in patients with long-persistent AF is associated with higher extent of atrial fibrosis (atrial DE), suggesting that fibrosis and electrical complexity increase in parallel with the duration of uninterrupted AF as the consequences of remodelling.

Spatial distribution of dense/continuous atrial delayed enhancement

Dense DE was consistently encountered on the left side of the posterior LA (adjacent to the left PV ostia and within the track/path of the descending aorta) in all patients (figure 1C&4). The predominance of fibrotic remodelling of the posterior LA has recently been reported using post-mortem histological analysis of the LA in patients with mitral valvular AF [7]. The consistent presence of dense DE in the left-sided posterior LA wall in all our patients may suggest higher shear/stretch forces in these region of LA.

CFAE, atrial delayed enhancement and ablation strategy

Our results demonstrate that a majority (48%) of continuous CFAE sites are not related to DE areas and occur at healthy atrial tissue (non-DE) without evidence of fibrosis on MRI. However, we found that 41% of continuous CFAE sites occur at patchy DE sites, with a lower content (37+/-12%) of DE, when compared to dense DE regions with a higher DE-content (96+/-4% regional enhancement). With the exception of organised electrical activity, that was observed more often at patchy DE regions than at non-DE sites, no significant electrical differences were notable between patchy DE and non-DE sites. However, 19+/-6% of CFAE sites do occur at border zones of or within the dense DE regions. This finding may be of importance. Ablative treatment of AF is more difficult in long-persistent AF, especially when the baseline AF cycle length is shorter than 150ms [19]. In these patients isolation of pulmonary veins needs to be followed by CFAE ablation and linear lesions to obtain higher rates of acute and long-term arrhythmia freedom. It has been recently shown that the ablation of continuous CFAE sites in persistent AF is associated with AF cycle length prolongation in about 50% of ablation attempts [4]. Importantly, in our current study we found 41% of continuous CFAE sites to occur at patchy DE areas, 11% of CFAE at dense DE areas and 48% of CFAE at healthy non-DE atrial regions. A recent study with high-density mapping of AF, revealed higher

bipolar voltage values at CFAE sites than at LA sites without CFAE, confirming our findings of inverse relationship between CFAE and atrial fibrosis (DE) [6]. In fact, recent studies have shown that at least 50% of CFAE sites are passive bystanders, e.g. due to non-local signals or wave collisions[6,12]. This study confirms that most continuous CFAE sites occur at healthy atrial sites. Thus, our results suggest that during CFAE ablation, we mostly target healthy (non-DE or patchy DE) tissue rather than fibrotic (dense DE) areas. Therefore, these data may be of clinical importance for the AF ablationist. Because of the limited specificity of CFAE sites as arrhythmia substrate in AF (only 50% of continuous CFAE sites will have impact on AF cycle length during ablation [4]) and most CFAE regions being healthy atrial tissue (without or with little evidence of fibrosis), CFAE ablation should be limited to regions, where further linear ablation may be needed (LA roof, inferior LA facing CS, mitral isthmus region and other cardiac veins as the CS) and to the atrial sites with rapid activity and local activation gradients. The present study used post-processing for initially time-consuming MR image processing (detection/segmentation of DE) for comparison with continuous CFAE sites. Therefore, we did not compare impact of ablation at specific CFAE sites (dense vs patchy DE regions) on AF cycle length or AF termination. However, we did ablate continuous CFAE sites in all 11 patients with long-persistent AF, which significantly prolonged AF cycle length (from mean 135 to 190ms, $p<0.05$) in 7/11 (64%) patients with long persistent AF.

CFAE in Atrial Fibrillation

The impact of atrial fibrosis on wave propagation has been studied in animal models of persistent AF [8]. With disease progression (short-persistent to long-persistent AF), it may be likely that an increasing amount of fibrosis (DE) within the atrial wall allows formation of a substrate favourable for slow conduction and re-entry of wavelets capable of perpetuating AF.

We observed that the patients with long-persisting AF and shorter AFCL had higher extent of atrial DE than patients with persistent AF and longer AFCL. Although dense DE sites display electrograms with lower voltage and slower cycle length instead of continuous CFAE, they may be important arrhythmia contributers in long-persistent AF. Dense DE regions may participate in perpetuating the arrhythmia by acting as boundaries critical to anchor rotors or transient re-entrant circuits. Alternatively, the re-entrant circuits may occur within or around the fibrotic areas.

Recently, simultaneous high-density endo- and epicardial mapping in human AF has shown dissociated/dyssynchronous activation of LA endo- and epicardium with distinct sites of breakthrough [14]. The endo- epicardial dissociation and dyssynchronous activation may also contribute to CFAE generation during AF. Our observation of more regular and non-fractionated electrical activity at dense DE regions may be explained by the absence of multiple layers of atrial muscle in dense DE regions. The CFAE within patchy DE and dense DE atrial regions may be the consequence of fibrosis-related slow conduction and/or endo-/epicardial dyssynchronous activity. Therefore, one can hypothesize that the CFAE sites in or around dense scar may represent preferential ablation targets in patients with persistent AF. Further studies would be needed to demonstrate that ablation targeting CFAE sites in or around dense scar allows for a more specific treatment of persistent AF.

Conclusions:

Using high-resolution, late-enhanced MRI for atrial fibrosis imaging and high density mapping during AF, we found most (48%) of the continuous CFAE sites at LA regions without any DE and 41% of CFAE at regions with lower content of delayed enhancement (patchy DE). Most (78%) of the dense DE sites did not display CFAE but slower, low-voltage

electrical activity. However, 19% of CFAE occur within or around dense DE sites. These findings may be of clinical importance for choosing the ablation strategy in patients with persistent AF. The region of slow conduction (with fractionated or rapid activity) within or around the areas of atrial fibrosis may be a promising ablation target in patients with persistent AF. Alternatively, novel global biatrial mapping systems are currently in clinical evaluation phase and will allow for a more mechanistically oriented ablation strategy in persistent AF, that target the patient specific AF sources and drivers [21-23].

Limitations:

1. DE-MRI resolution: The thickness of LA wall varies from 1mm to 7 mm. LA regions with wall thickness of 1mm are below the resolution of currently used MRI. With further advances in MRI-based fibrosis imaging (use of higher magnetic field gradients (3T instead of 1,5 Tesla) with better signal to noise ratio and T1-T2 imaging), it would be interesting to assess the transmurality of atrial fibrosis.

2. Dense DE areas were electrically distinct from patchy DE or non-DE LA sites. However, mapping with a 20-pole catheter (1mm electrodes, spacing 4mm), we could not electrically distinguish (with the exception of electrogram organisation, 6B) between patchy DE regions and non-DE areas. High-resolution, simultaneous whole-chamber mapping with more advanced mapping tools may allow deeper and better understanding of wave propagation during AF and the impact of atrial fibrosis on pro-arrhythmia.

MRI resolution for fibrosis detection is limited. It is possible that patchy DE sites with intermittent DE, may partly be due to MRI “noise” detection. In that case, some of patchy DE sites might even be healthier and not contain any fibrosis.

Funding Sources:

The research leading to these results has received funding from the European Union Seventh Framework Programme (FP7/2007-2013) under Grant Agreement HEALTH-F2-2010-261057.

Acknowledgement:

Dr A Jadidi received a research grant from Hopitaux Universitaire de Geneve and SJM.

Disclosures: None.

References

(1) Haissaguerre M, Jais P, Shah DC, et al. Spontaneous initiation of atrial fibrillation by ectopic beats originating in the pulmonary veins. *N Engl J Med* 1998;339:659-66.

(2) Jais P, Haissaguerre M, Shah DC, et al. Regional disparities of endocardial atrial activation in paroxysmal atrial fibrillation. *Pacing Clin Electrophysiol* 1996;19:1998-2003.

(3) Nademanee K, McKenzie J, Kosar E, et al. A new approach for catheter ablation of atrial fibrillation: mapping of the electrophysiologic substrate. *J Am Coll Cardiol* 2004;43:2044-53.

(4) Takahashi Y, O'Neill MD, Hocini M, et al. Characterization of electrograms associated with termination of chronic atrial fibrillation by catheter ablation. *J Am Coll Cardiol* 2008;51:1003-10.

(5) Konings KT, Kirchhof CJ, Smeets JR, et al. High-density mapping of electrically induced atrial fibrillation in humans. *Circulation*;89:1665-80.

(6) Jadidi AS, Duncan E, Miyazaki S, et al. Functional nature of electrogram fractionation demonstrated by left atrial high-density mapping. *Circ Arrhythm Electrophysiol* 2012;5:32-42.

(7) Corradi D, Callegari S, Benussi S, et al. Myocyte changes and their left atrial distribution in patients with chronic atrial fibrillation related to mitral valve disease. *Hum Pathol* 2005;36:1080-9.

(8) Tanaka K, Zlochiver S, Vikstrom KL, et al. Spatial distribution of fibrosis governs fibrillation wave dynamics in the posterior left atrium during heart failure. *Circ Res* 2007;101:839-47.

(9) Oakes RS, Badger TJ, Kholmovski EG, et al. Detection and quantification of left atrial structural remodeling with delayed-enhancement magnetic resonance imaging in patients with atrial fibrillation. *Circulation* 2009;119:1758-67.

(10) Daccarett M, Badger TJ, Akoum N, et al. Association of left atrial fibrosis detected by delayed-enhancement magnetic resonance imaging and the risk of stroke in patients with atrial fibrillation. *J Am Coll Cardiol* 2011;57:831-8.

(11) Tsai WC, Lin YJ, Tsao HM, et al. The Optimal Automatic Algorithm for the Mapping of Complex Fractionated Atrial Electrograms in Patients With Atrial Fibrillation. *J Cardiovasc Electrophysiol* 2009;21:21-26.

(12) Narayan SM, Wright M, Derval N, et al. Classifying fractionated electrograms in human atrial fibrillation using monophasic action potentials and activation mapping: Evidence for localized drivers, rate acceleration, and nonlocal signal etiologies. *Heart Rhythm* 2011;8:244-53.

(13) Wijnmaalen AP, van der Geest RJ, van Huls van Taxis CF, et al. Head-to-head comparison of contrast-enhanced magnetic resonance imaging and electroanatomical voltage mapping to assess post-infarct scar characteristics in patients with VTs: real-time image integration and reversed registration. *Eur Heart J* 2011 January;32:104-14.

(14) Allessie MA, de Groot NM, Houben RP, et al. Electropathological substrate of long-standing persistent atrial fibrillation in patients with structural heart disease: longitudinal dissociation. *Circ Arrhythm Electrophysiol* 2010;3:606-15.

(15) Jacques M.T. de Bakker, F.Wittkampf. The Pathophysiologic Basis of Fractionated and Complex Electrograms and the Impact of Recording Techniques on Their Detection and Interpretation. *Circ Arrhythm Electrophysiol* 2010;3:204-213.

(16) Spach MS, Heidlage JF, Dolber PC, et al. Mechanism of origin of conduction disturbances in aging human atrial bundles: experimental and model study. *Heart Rhythm*. 2007; 4:175-85.

(17) Zlochiver S, Yamazaki M, Kalifa J, et al. Rotor meandering contributes to

irregularity in electrograms during atrial fibrillation. *Heart Rhythm.* 2008; 5: 846–854.

(18) Lin J, Scherlag BJ, Zhou J, et al. Autonomic mechanism to explain complex fractionated atrial electrograms. *J Cardiovasc Electrophysiol.* 2007;18:1197-205.

(19) Haissaguerre M, Lim KT, Jacquemet V, et al. Atrial fibrillatory cycle length: computer simulation and potential clinical importance. *Europace.* 2007;9:64-70.

(20) Kawara T, Derksen R, de Groot JR, et al. Activation delay after premature stimulation in chronically diseased human myocardium relates to the architecture of interstitial fibrosis. *Circulation.* 2001;104:3069-75.

(21) Cuculich PS, Wang Y, Lindsay BD, et al. Noninvasive Characterization of Epicardial Activation in Humans with Diverse Atrial Fibrillation Patterns. *Circulation.* 2010; 122:1364-1372.

(22) Narayan SM, Krummen DE, Shivkumar K, et al. CONFIRM (Conventional Ablation for Atrial Fibrillation With or Without Focal Impulse and Rotor Modulation) Trial. *JACC.* 2012;60:628-36.

(23) Haissaguerre M, Hocini M, Shah A, et al. Noninvasive Panoramic Mapping of Human Atrial Fibrillation Mechanisms - A feasibility report. *JCE 2012 Dec 17. doi: 10.1111/jce.12075*

Table 1: Clinical Characteristics of Study Population (n=18)

Age (years)	63 ± 7
Sex (male/female)	16/2
History of AF (months)	81 ± 65
Duration of Continuous AF (months)	25 ± 27
Long Persistent AF (>12 month)	11

LVEF (%)	53 ± 13
Left Ventricular dysfunction (LVEF<50%) (n)	9
LVEDD (mm)	54 ± 7
LVESD (mm)	36 ± 9
IVSDD (mm)	12+/-2
LAD (mm)	46 ± 7
Structural Heart Disease	7
Coronary Artery Disease	1
Hypertension	13
Number of failed AAD	2.4 ± 1.0
Administration of amiodarone	12
Number of electrical cardioversions	1.8 ± 0.8
Left Atrial Appendage Cycle length	153+/-15ms

AF = atrial fibrillation; LVEF = left ventricular ejection fraction; LVEDD = left ventricular end diastolic diameter; LVESD = left ventricular end systolic diameter; IVSDD =inter ventricular septum diastolic diameter; LAD = Left Atrial Diameter (antero-posterior); AAD = antiarrhythmic drug

Table 2. Comparison Characteristics in patients with persistent (>7days) and long-persistent (>12 months of continuous AF) AF

	Long-Persistent AF (n=11)	**Persistent AF (n=7)**	**P-Value**

Age (years)	64 ± 9	59 ± 8	0.13
Sex (male/female)	10/1	7/0	0.43
History of AF (months)	86 ± 61	78 ± 71	0.90
Duration of Continuous AF (months)	25 ± 8	2 ± 1	**0.02**
LVEF (%)	48 ± 11	57 ± 9	0.07
Total left atrial surface area (cm2)	134+/-38	98+/-9	**0.02**
Extent of Atrial DE (cm2)	69.5+/-15.6	48.5+/-9.6	**0.01**
Extent of continuous CFAE (cm2)	54+/-16	28+/-15	**0.02**
Left Ventricular dysfunction (LVEF<50%) (n)	4	2	0.17
LVEDD	59 ± 6	55 ± 4	
IVSD	12± 1	11± 2	0.73
LAD (mm)	49 ± 5	43 ± 4	0.06
Structural Heart Disease	6	1	0.08
Coronary Disease	1	0	0.53
Hypertension	8	5	0.42
Number of failed AAD	2.1± 1.0	1.7 ± 1.0	0.38
Administration of amiodarone	10/11	6/7	0.52
Number of DCCV	2.1 ± 0.9	1.6 ± 0.7	0.58
LAA Baseline AFCL (ms)	147 ± 10	182 ± 16	**0.01**

Figure legends:

Figure 1A-E: Figure 1 A-E: Detection, segmentation and 3-dimensional reconstruction of atrial delayed enhancement (DE). High resolution (1.25x1.25x2.5mm) DE-MRI (1A). 1B: Segmentation of LA wall between the inner (red) and outer (green) markers. 1D: Voxel intensity histogram analysis of LA wall identifies DE as voxel intensities >4SD than the median in-plane voxel intensity. 1C: Regions of DE are depicted in yellow. 1E: 3-D-reconstruction of LA blood pool and DE areas. Dense DE regions are measured using the red marker in 1E with corresponding red arrows in 1C, and patchy DE regions are measured using the green marker in 1E with corresponding green arrows in 1C.

Figure 2 A-C: Relationship between LA size, total atrial DE, AF cycle length and extent of continuous CFAE in patients with long-persistent and persistent AF. 2A: Long-persistent AF patients have larger LA size, higher extent of total atrial DE, larger extent of continuous CFAE regions and shorter AF cycle length. **2B:** Patients with shorter baseline AFCL have higher extent of aDE. **2C:** An inverse correlation exists between extent of aDE and AF cycle length. Dots represent values of single patients.

Figure 3A: Quantitative assessment of LA size, extent of continuous CFAE and atrial DE regions.

Figure 3 B-E: Distribution and relationship of CFAE surfaces to DE regions. Continuous CFAE occupied 38+/-19% of LA surface (3B). Dense DE took 14+/-5% and patchy DE 43+/-12% of the LA surface (3C). Most CFAE (48+/-14%) occurred at non-DE, followed by patchy (41+/-12%) and dense (11+/-6%) DE sites (3D). 23+/-13% of dense DE, 35+/-18% of patchy DE and 46+/-27% of non-DE region displayed CFAE (3E).

Figure 4A-D: Relationship of atrial DE to continuous CFAE sites. Examples showing relationship between dense DE, patchy DE and continuous CFAE sites (CFEmean <80ms) from 2 patients with long-persistent AF. Continuous CFAE occupy 38+/-19% of total LA surface. Most CFAE (48+/-14%) occur at non-DE followed by 41+/-12% at patchy DE areas. A minority of CFAE (11+/-6%) occurs at dense DE areas. Dense DE areas display slower and more organized electrical activity than elsewhere (see electrograms in green box, figure 4B and D).

Figure 5A-B: Degree of Fractionation at dense DE vs patchy DE vs non-DE regions. Degree of electrogram fractionation was lower with higher CFEmean intervals at dense DE (108+/-44ms; median: 97.1ms) vs. patchy DE (87+/-34ms; median: 75.8ms, $p<0.0001$) and non-DE sites (85.7+/-32ms; median: 75.8ms, $p<0.0001$; figure 5A). Histogram analysis of CFEmean at dense DE vs. patchy DE and non-DE regions (5B) : Continuous CFAE (CFEmean <80ms) constituted about 57% of Egms recorded within patchy DE or non-DE regions (green and pink) vs. <33% in dense DE regions ($p=0.009$, 5B).

Figure 6A-C: Electrogram Cycle length (6A), organized activity (6B) and bipolar voltage (6C) between dense DE vs patchy DE vs non-DE sites: Dense DE sites showed slower and more organized electrical activity with lower mean bipolar voltage during AF than other LA sites (6A,B&C).

Detection, Segmentation & 3D-Reconstruction of atrial delayed enhancement

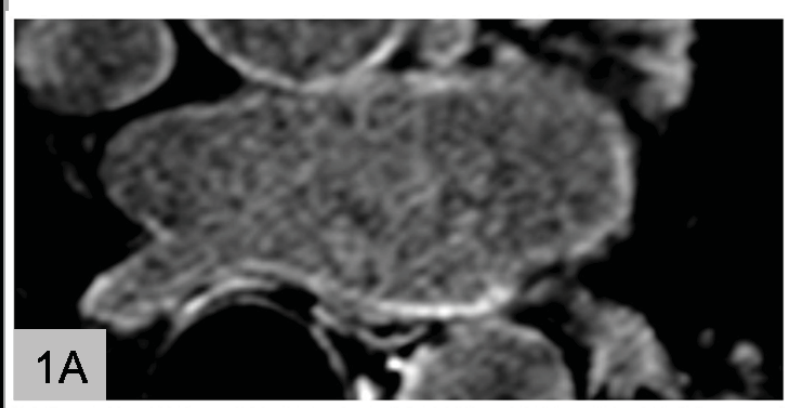

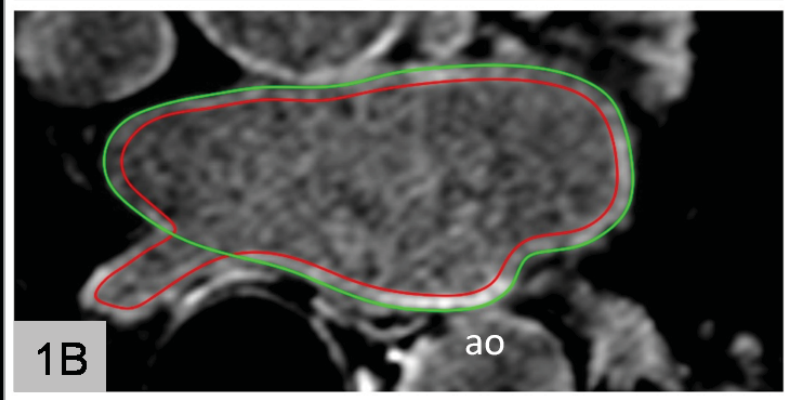

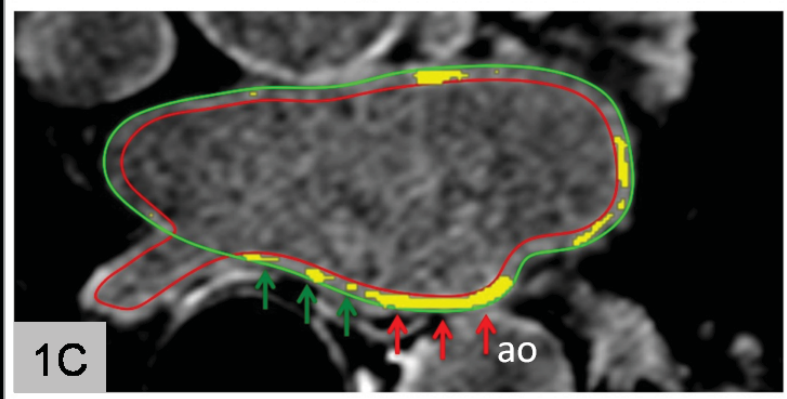

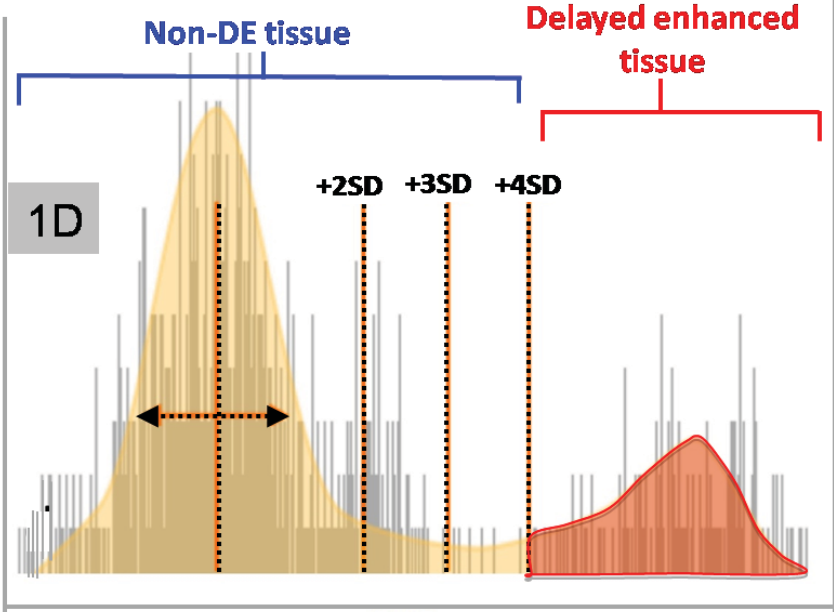

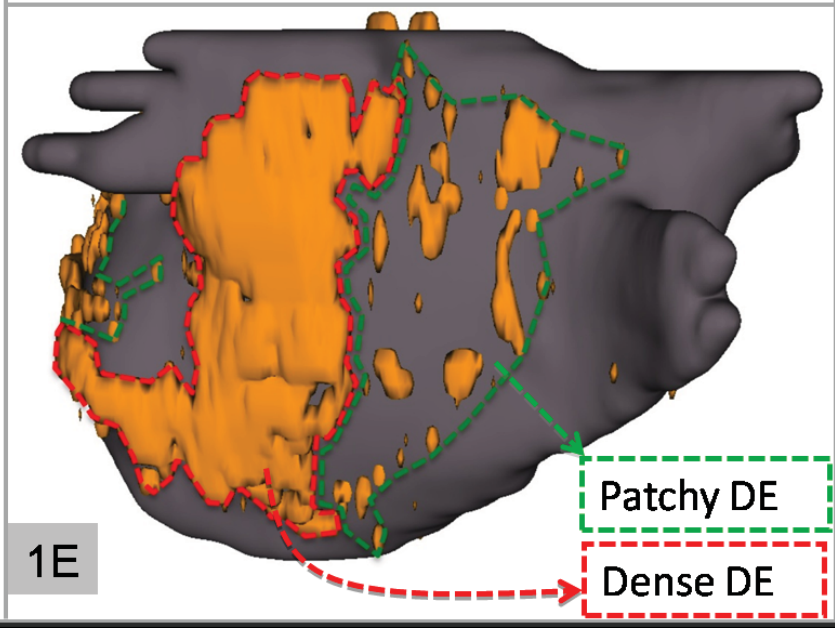

Long-Persistent AF displays higher Extent of DE and CFAE with shorter AF Cycle Length

2A

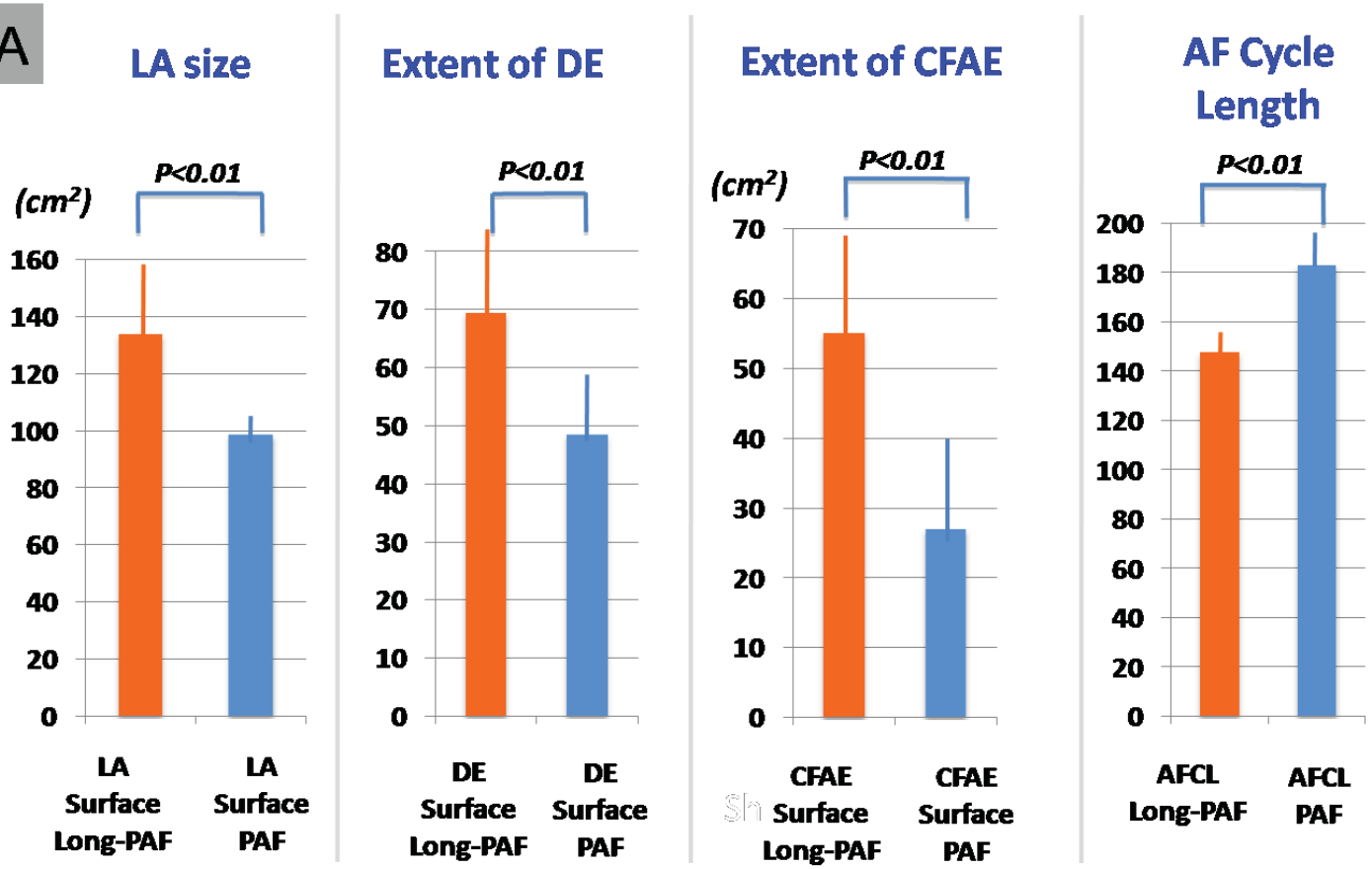

Shorter AFCL is associated with increased amount of DE

2B

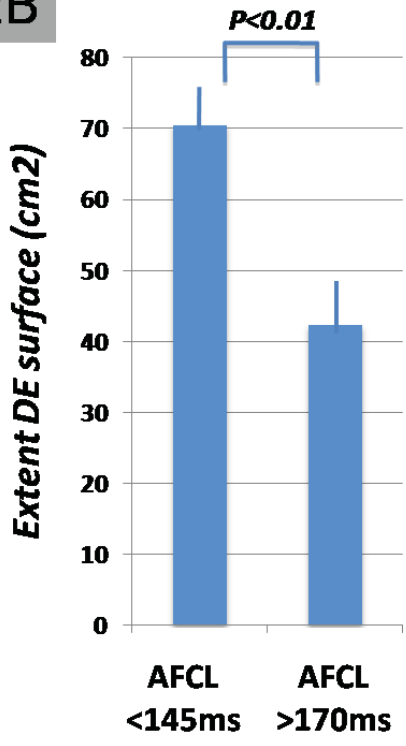

2C

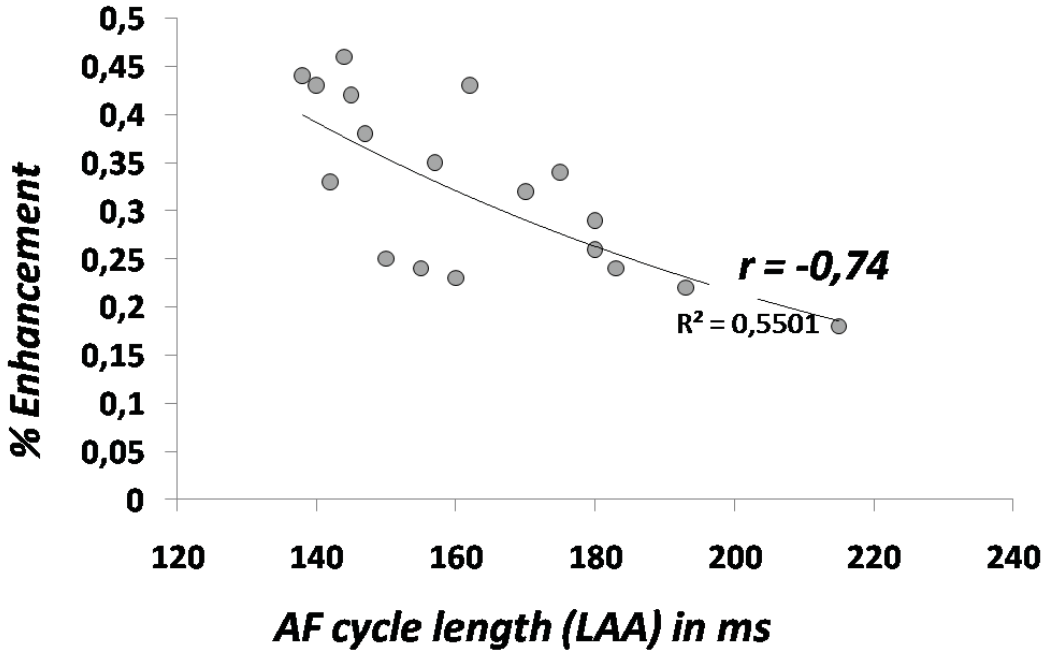

3A

LA Size, CFAE surface and DE surfaces in total Study Population

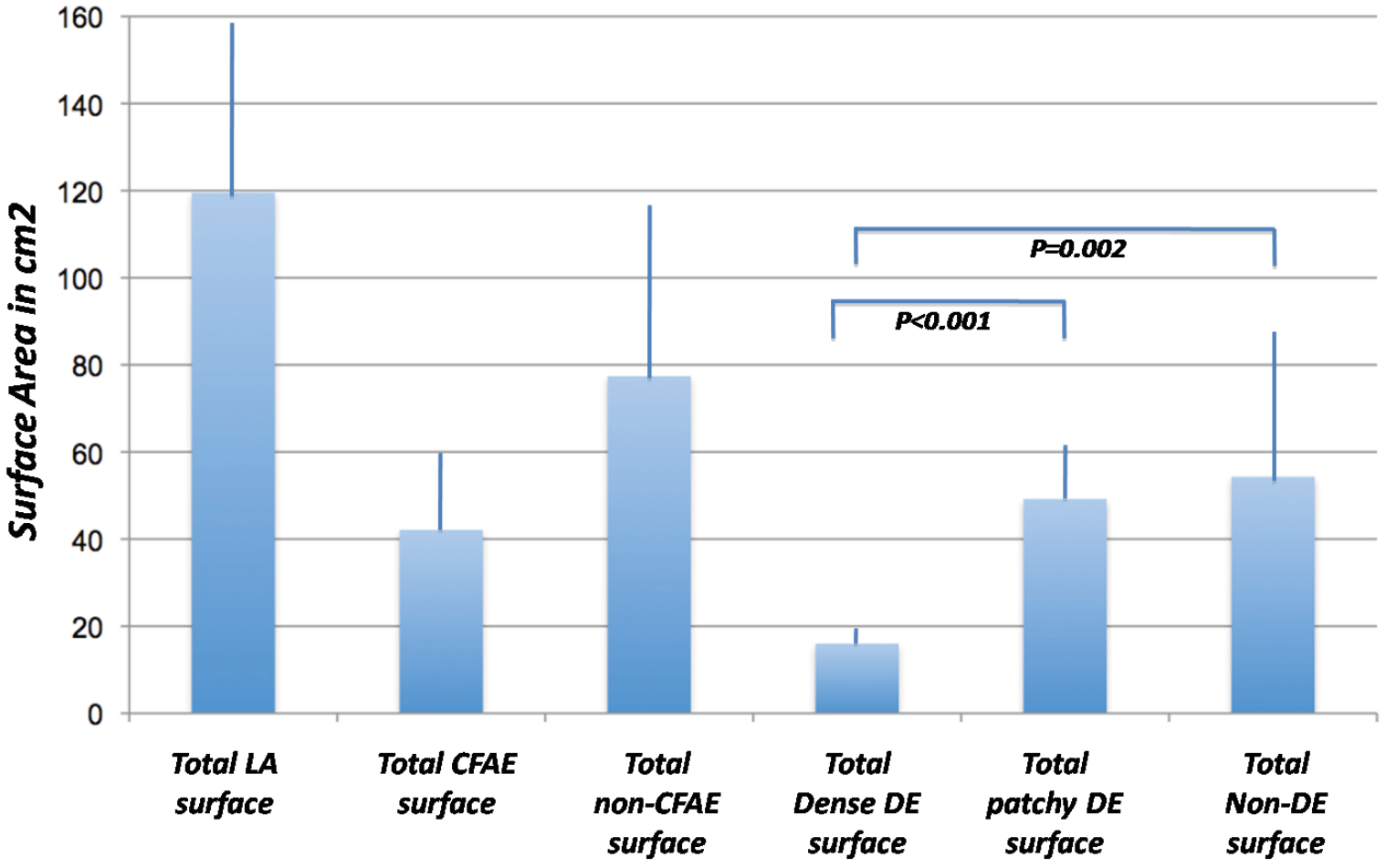

Distribution and Relationship of CFAE Surfaces to Delayed Enhanced Atrial Regions

3B CFAE as a Percentage of LA Surface

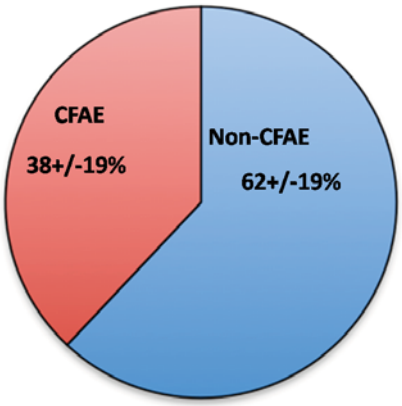

3C DE as a Percentage of LA Surface

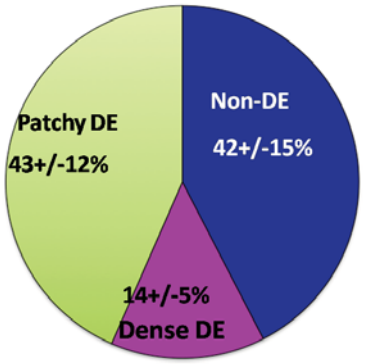

3D DE as Percentage of CFAE

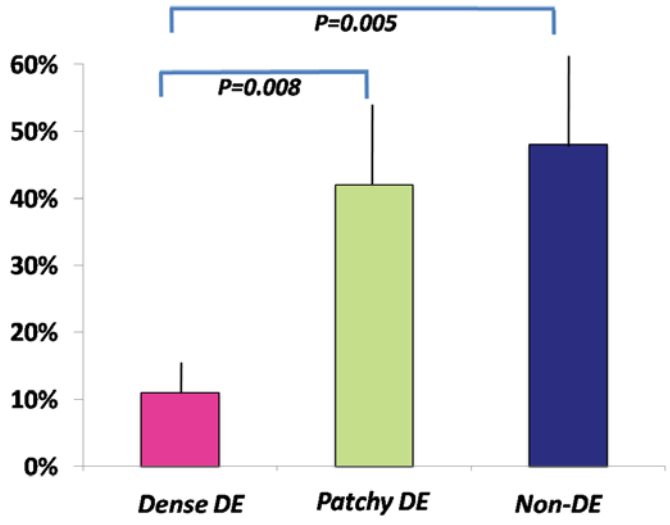

3E CFAE as Percentage of DE Region

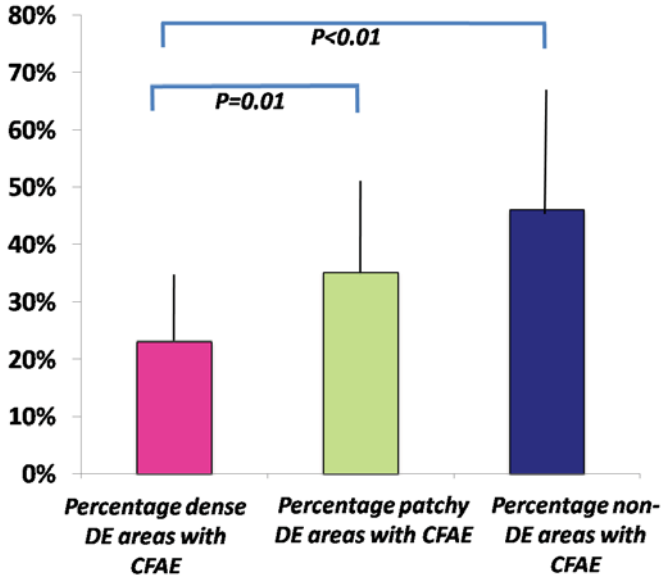

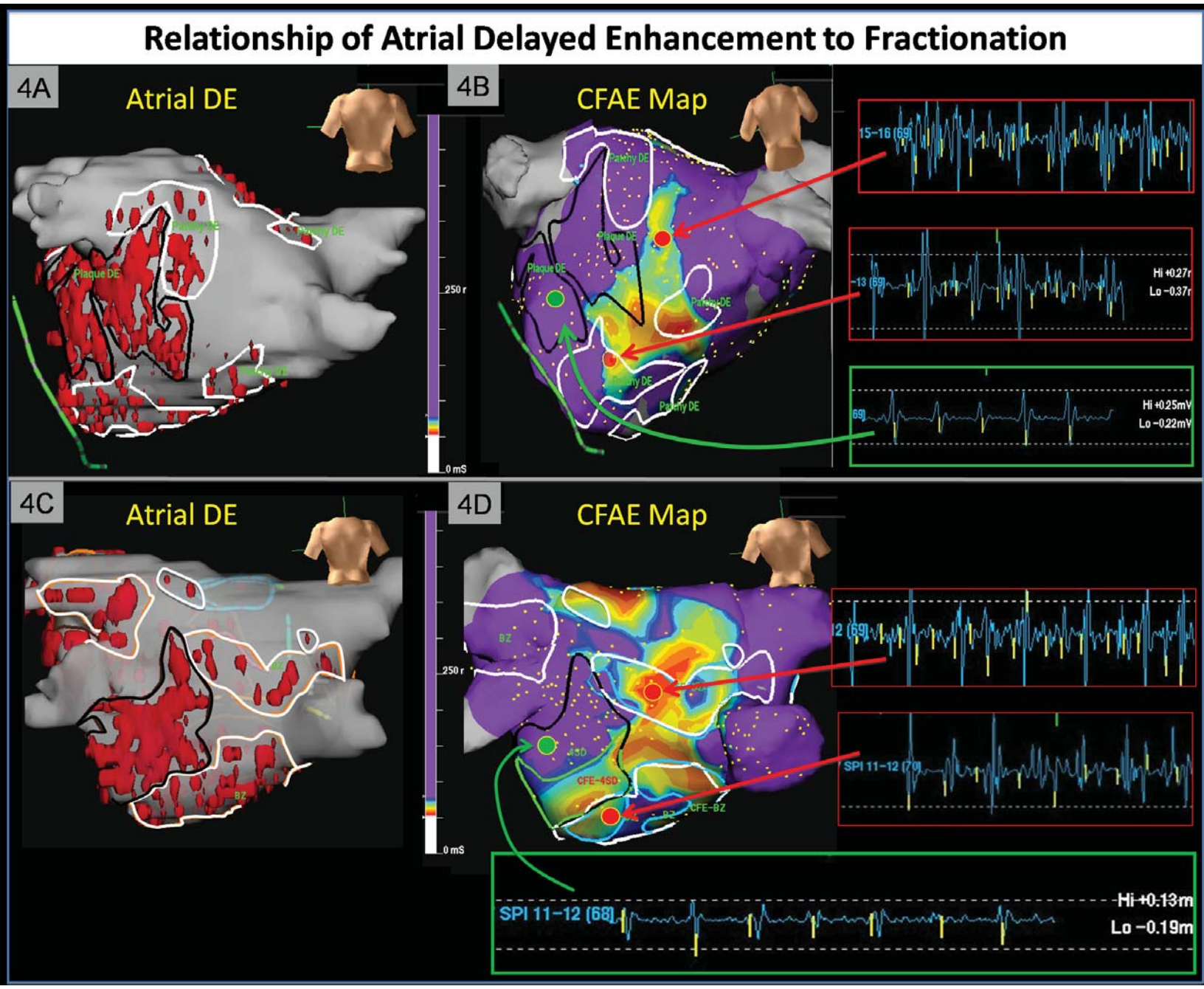
Relationship of Atrial Delayed Enhancement to Fractionation
4A
Atrial DE
Plaque DE
Patchy DE
4B
CFAE Map
Plaque DE
Patchy DE
250 r
0 mS
15–16 (69)
Hi +0.27r
Lo −0.37r
Hi +0.25mV
Lo −0.22mV
4C
Atrial DE
BZ
4D
CFAE Map
BZ
CFE–4SD
CFE–BZ
250 r
0 mS
SPI 11–12 (68)
Hi +0.13m
Lo −0.19m

5A

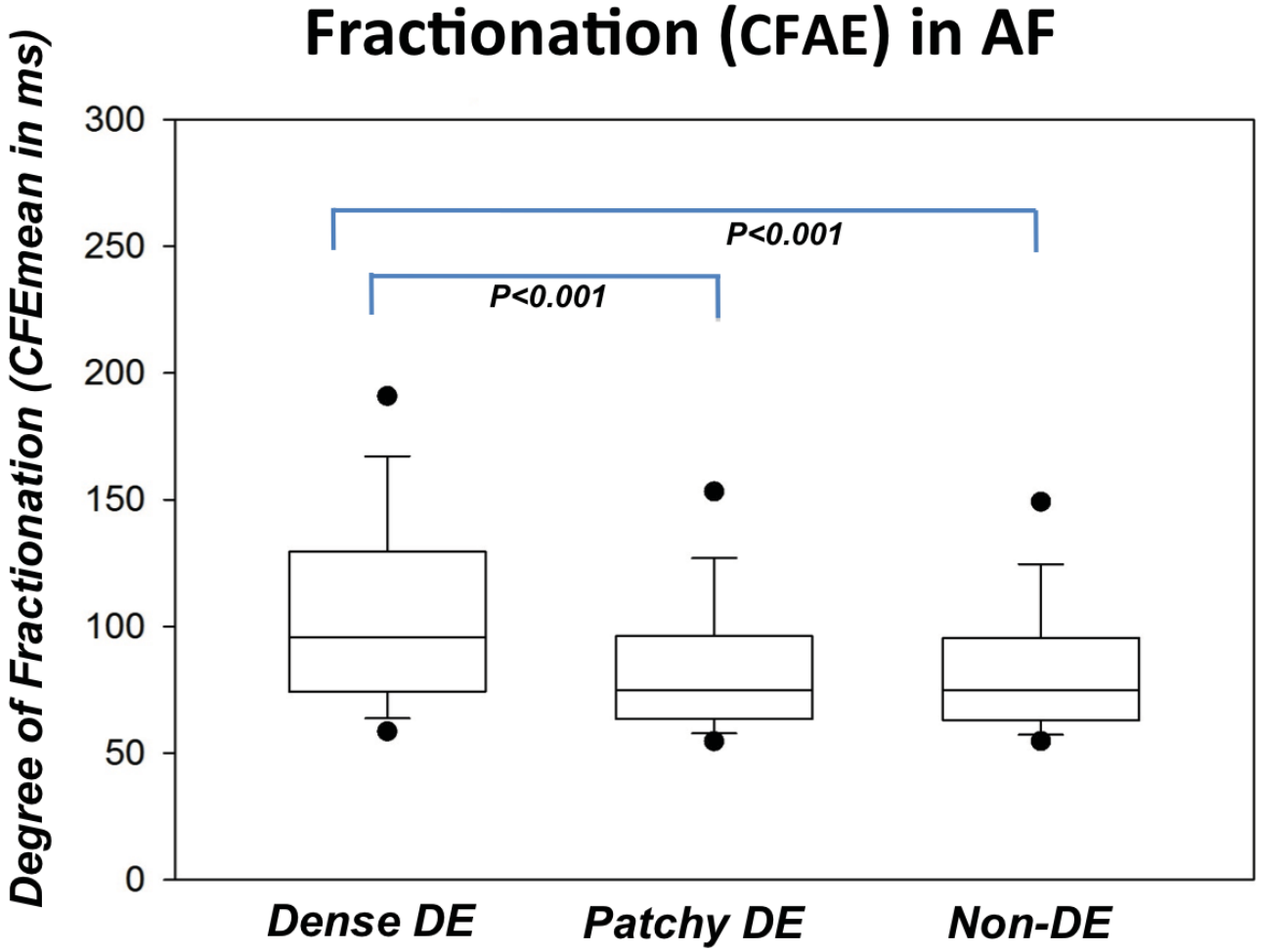
Fractionation (CFAE) in AF
Degree of Fractionation (CFEmean in ms)
300
250
200
150
100
50
0
P<0.001
P<0.001
Dense DE
Patchy DE
Non-DE

5B

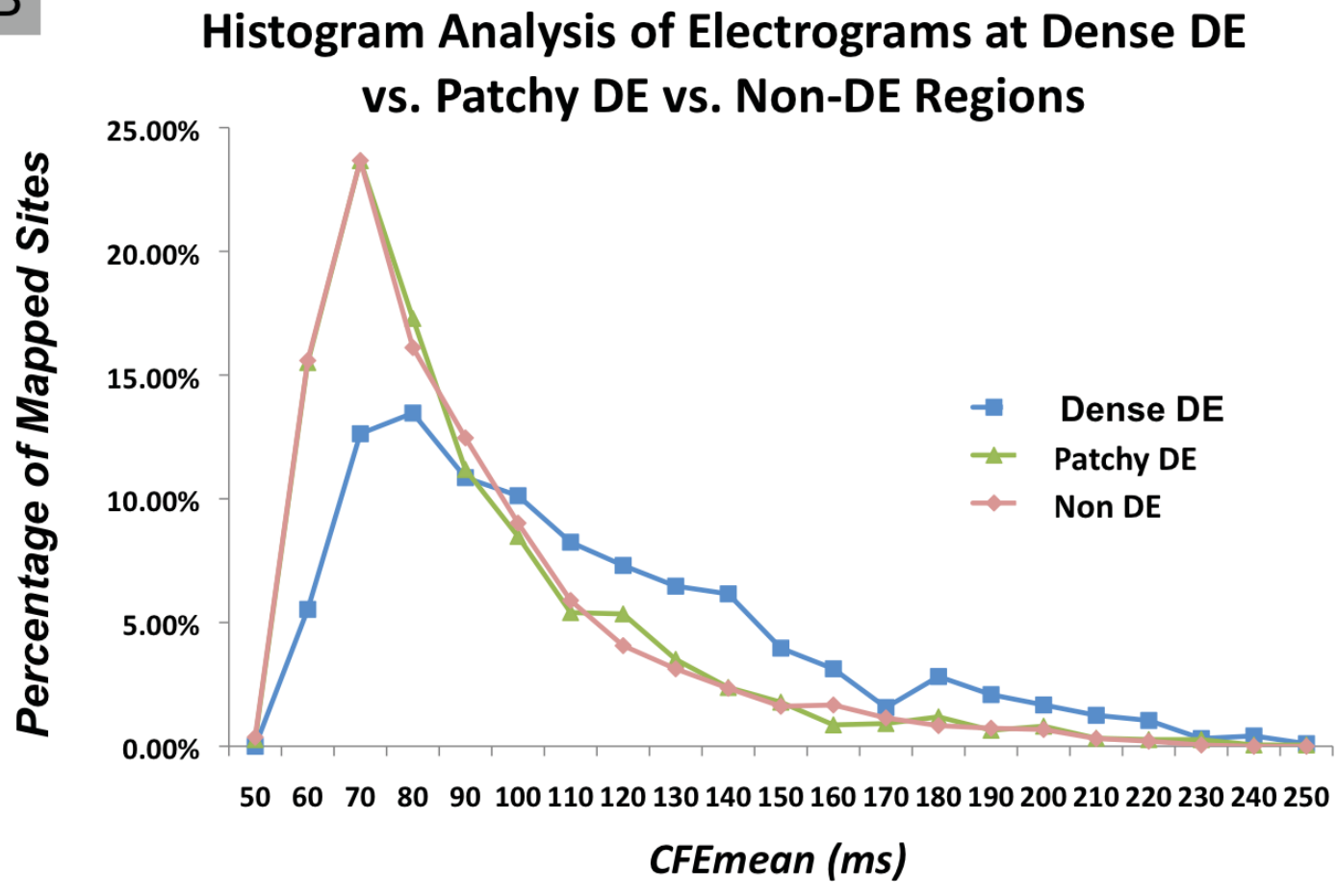
Histogram Analysis of Electrograms at Dense DE vs. Patchy DE vs. Non-DE Regions
Percentage of Mapped Sites
25.00%
20.00%
15.00%
10.00%
5.00%
0.00%
Dense DE
Patchy DE
Non DE
50 60 70 80 90 100 110 120 130 140 150 160 170 180 190 200 210 220 230 240 250
CFEmean (ms)

6A

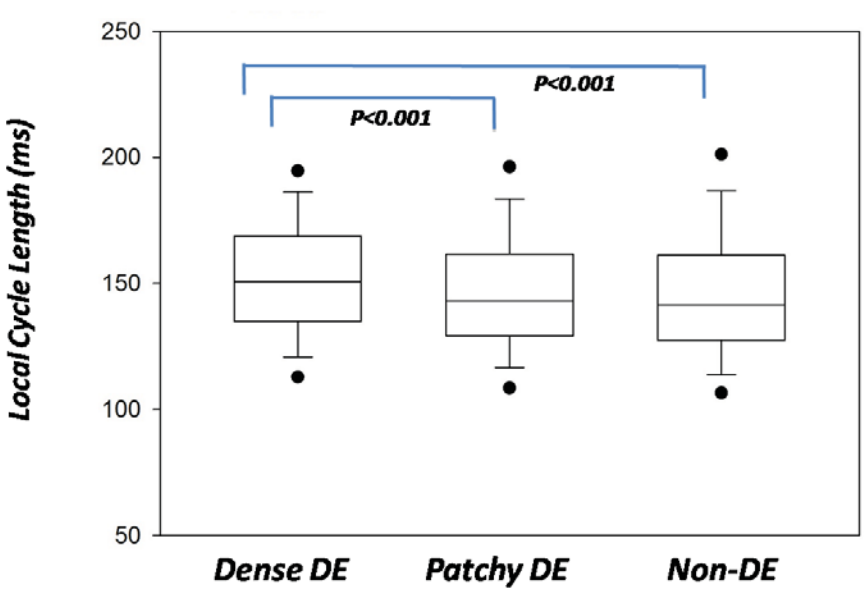
Local Mean Cycle Length in AF
Local Cycle Length (ms)
250
200
150
100
50
P<0.001
P<0.001
Dense DE
Patchy DE
Non-DE

6B

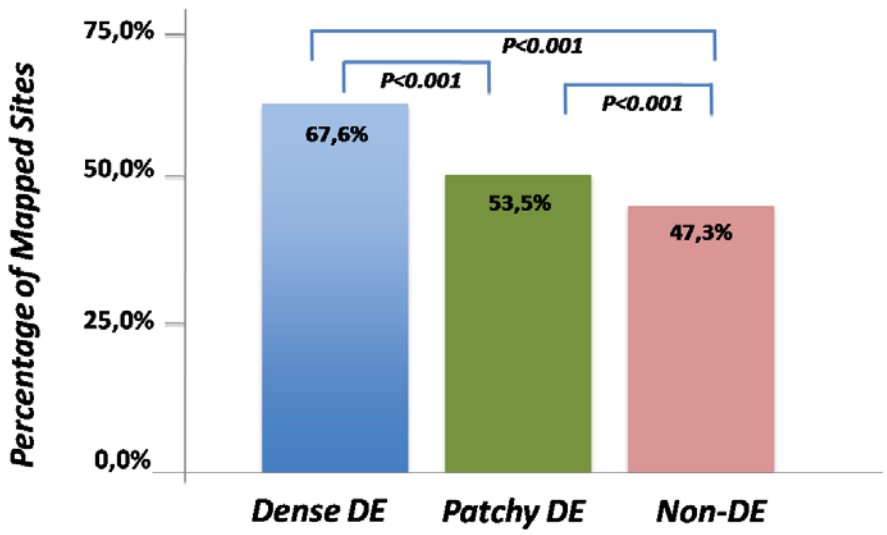
Percentage of Organized Mapping Sites
Percentage of Mapped Sites
75,0%
50,0%
25,0%
0,0%
P<0.001
P<0.001
P<0.001
67,6%
53,5%
47,3%
Dense DE
Patchy DE
Non-DE

6C

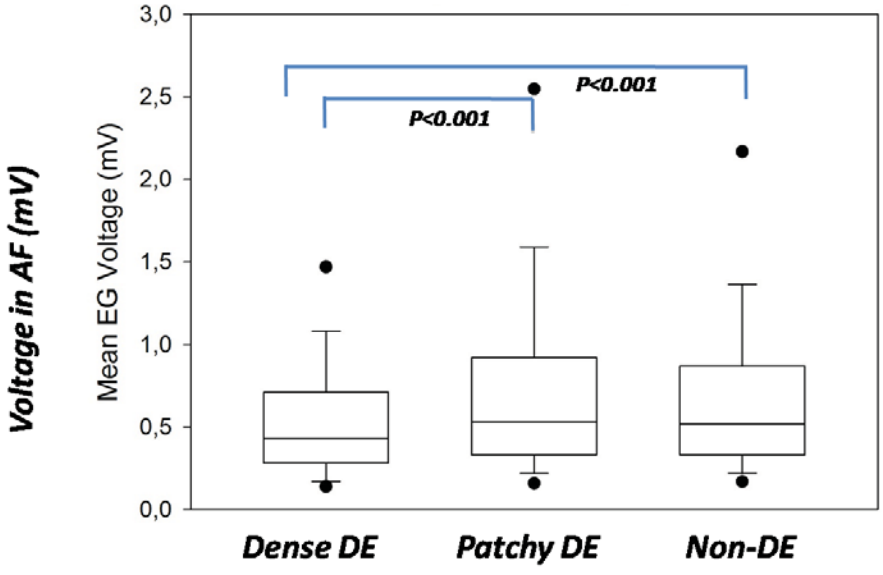
Electrogram Voltage in AF
Voltage in AF (mV)
Mean EG Voltage (mV)
3,0
2,5
2,0
1,5
1,0
0,5
0,0
P<0.001
P<0.001
Dense DE
Patchy DE
Non-DE